Oncogene (2005) 24, 5355–5364

www.nature.com/onc

The merlin tumor suppressor interacts with Ral guanine nucleotide dissociation stimulator and inhibits its activity

Chung Hun Ryu[1,2], Sae-Woong Kim[2], Kyu Hwa Lee[1], Joo Yong Lee[1], Hongtae Kim[1], Woon Kyu Lee[3], Byung Hyune Choi[1], Young Lim[4], Young Hoon Kim[1], Kweon-Haeng Lee[3], Tae-Kon Hwang[2], Tae-Youn Jun*[,1,5] and Hyoung Kyun Rha[1]

[1]*Catholic Neuroscience Center, The Catholic University of Korea, Seoul 137-701, Korea;* [2]*Department of Urology, The Catholic University of Korea, Seoul 137-701, Korea;* [3]*Department of Pharmacology, The Catholic University of Korea, Seoul 137-701, Korea;* [4]*Department of Occupational and Environmental Medicine, The Catholic University of Korea, Seoul 137-701, Korea;* [5]*Department of Psychiatry, The Catholic University of Korea, Seoul 137-701, Korea*

Neurofibromatosis type 2 (*NF2*) is the most commonly mutated gene in benign tumors of the human nervous system such as schwannomas and meningiomas. The *NF2* gene encodes a protein called schwannomin or merlin, which is involved in regulating cell growth and proliferation through protein–protein interactions with various cellular proteins. In order to better understand the mechanism by which merlin exerts its function, yeast two-hybrid screening was performed and Ral guanine nucleotide dissociation stimulator (RalGDS), a downstream molecule of Ras, was identified as a merlin-binding protein. The direct interaction between merlin and RalGDS was confirmed both *in vitro* and in the NIH3T3 cells. The domain analyses revealed that the broad C-terminal region of merlin (aa 141–595) is necessary for the interaction with the C-terminal Ras-binding domain (RBD) of RalGDS. Functional studies showed that merlin inhibits the RalGDS-induced RalA activation, the colony formation and the cell migration in mammalian cells. These results suggest that merlin can function as a tumor suppressor by inhibiting the RalGDS-mediated oncogenic signals.
Oncogene (2005) **24,** 5355–5364. doi:10.1038/sj.onc.1208633; published online 27 June 2005

Keywords: NF2; merlin; tumor suppressor; RalGDS; oncogenic signals

Introduction

Neurofibromatosis type 2 (NF2) is a dominantly inherited disorder that predisposes patients to the development of multiple benign tumors of the human nervous system such as schwannomas and meningiomas (Thomas *et al*., 1994; Louis *et al*., 1995). The *NF2* gene product is referred to as either merlin or schwannomin, and has a sequence homology to the members of the 4.1 family proteins such as ezrin, radixin and moesin (ERM proteins), which link the cytoskeleton to the plasma membrane (Rouleau *et al*., 1993; Trofatter *et al*., 1993). The ERM proteins have been implicated in the cellular remodeling and the formation of membrane microvilli and ruffles (Tsukita *et al*., 1997). Based on the sequence homology with the ERM proteins, merlin is also believed to function as a protein linking the cellular membrane and cytoskeleton. However, merlin has distinct properties and functions in the regulation of cell growth and proliferation that are not ascribed to ERM proteins (Shermn *et al*., 1997; Ikeda *et al*., 1999; Morrison *et al*., 2001).

In efforts to determine the cellular function of merlin, several groups have identified potential merlin-interacting proteins such as schwannomin interacting protein 1 (SCHIP-1), Na^+–H^+ exchanger regulatory factor (NHERF), βII-spectrine (also known as fodrin), CD44, synthenin, paxillin, hepatocyte growth factor-regulated tyrosine kinase substrate (HRS) (also known as HGS), merlin-associated protein (MAP) and trans-activation-responsive RNA-binding protein (TRBP) (Sainio *et al*., 1997; Murthy *et al*., 1998; Scoles *et al*., 1998; Goutebroze *et al*., 2000; Scoles *et al*., 2000; Jannatipur *et al*., 2001; Fernandez-Valle *et al*., 2002; Lee IK *et al*., 2004; Lee JY *et al*., 2004). These proteins are mostly associated with and involved in the function of the cellular membrane. Therefore, merlin might exert its tumor suppressor effects presumably by modulating the membrane receptor–cytoskeletal linkage that is essential for cell growth and the adhesion pathways via the interaction with these proteins (Koga *et al*., 1998; Jannatipur *et al*., 2001). However, the action mechanism of merlin as a tumor suppressor is still not fully understood just with the current reports.

In order to identify the novel proteins important in the function of merlin, yeast two-hybrid screening was performed with human brain cDNA library and merlin protein as bait. One of the positive clones encoded RalGDS, which functions as a Ras effector and a

*Correspondence: T-Y Jun, Department of Psychiatry, The Catholic University of Korea, 505 Banpo dong, Socho ku, Seoul 137-701, Korea; E-mail: ngrc@catholic.ac.kr
Received 17 November 2004; revised 7 February 2005; accepted 14 February 2005; published online 27 June 2005

GDP/GTP exchange factor (GEF) for the Ral protein (Rusanescu *et al*., 2001).

The activation of RalGDS and its target, Ral, constitutes a distinct downstream signaling pathway of the oncogenic Ras-induced cell transformation (McCormick and Wittinghofer, 1996; Joneson and Bar-Sagi, 1997; Vojtk and Der, 1998). In addition, similar to the active form of Ha-Ras, the constitutive active RalGDS mutant synergizes with Raf-1 to induce a transformation of NIH3T3 cells, which is inhibited by the dominant-negative mutant of RalA (Urano *et al*., 1996; White *et al*., 1996). Interestingly, many research groups have reported that the merlin tumor suppressor inhibits the Ras signaling pathways and the Ras-induced cell transformation (Tikoo *et al*., 1994; Kim H *et al*., 2002). Therefore, the interaction between RalGDS and merlin might negatively regulate the Ras–RalGDS–Ral signaling pathways and provide one of mechanisms of merlin as a tumor suppressor.

This report demonstrates the direct interaction of RalGDS and merlin both *in vitro* and *in vivo*, and presents evidence for the functional importance of their interaction.

Results

Identification of RalGDS as a merlin-binding protein

In order to identify the binding partner of merlin, the full length of merlin was used as bait for the yeast two-hybrid screening with a human brain cDNA library. Among 2×10^6 transformants, 25 strong positives were isolated and tested by a re-transformation. The partial nucleotide sequencing of the cDNA fragments revealed that four clones encoded the C-terminal portion of RalGDS. The full-length open reading frame of RalGDS was obtained using the 5′-RACE screening of the human placenta cDNA.

In order to map the RalGDS-interaction domain of merlin, the GAL4–DBD fused full-length and deletion derivatives of merlin were tested for the binding with the GAL4-AD fused full-length or the partial RalGDS (RalGDS-P) protein in the yeast two-hybrid system (Figure 1a). The yeast growth test showed that both the full-length and RalGDS-P actively interacted with the M1, M3 and M4 deletion mutants of merlin, but not with the M2 mutant that does not contain a Blue Box (BB) (Johnson *et al*., 2002; Sun *et al*., 2002). The β-galactosidase assays showed a consistent result but also revealed that RalGDS interacted only weakly with the M3 and M4 merlin mutants (Figure 1b). Overall, these results suggest that the broad C-terminal region (amino acids (aa) 141–595) of merlin is necessary for the full interaction with the C-terminal region of RalGDS, containing a RBD.

Merlin is associated with RalGDS in vitro *and in mammalian cells*

In order to confirm the direct interaction between RalGDS and merlin, the GST pull-down assays were performed using the GST–RalGDS fusion protein and the ^{35}S-labeled wild-type or mutant merlin proteins produced by *in vitro* translation. The result showed that the full-length merlin and only the M1 mutant among its four deletion mutants bound specifically to GST–RalGDS immobilized on the glutathione-Sepharose 4B beads (Figure 2). These results suggest that merlin interacts with RalGDS *in vitro* and confirmed that the 141–595 amino-acid region of merlin is necessary for this interaction. We speculate that the interaction

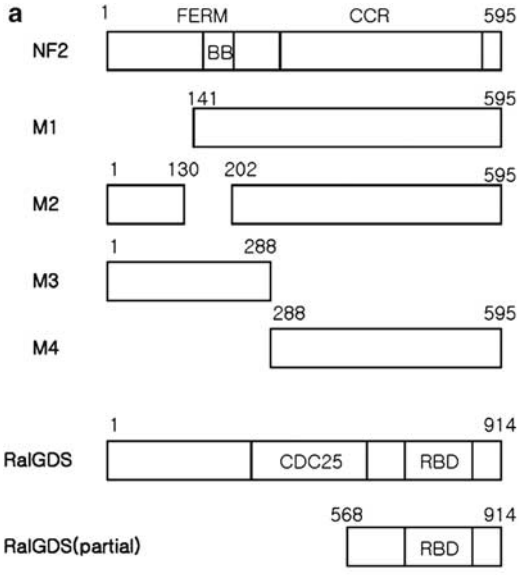

b

Bait	Prey	Yeast Growth	lacZ reporter activity
NF2	RalGDS	+	+++
M1	RalGDS	+	+++
M2	RalGDS	−	−
M3	RalGDS	+	+
M4	RAlGDS	+	+
NF2	RalGDS–P	+	+++
M1	RalGDS–P	+	+++
M2	RalGDS–P	−	−
M3	RalGDS–P	+	+
M4	RalGDS–P	+	+

β–galactosidase activity was scord as +++ (deep blue), ++ (intermediate blue), + (blue), − (white)

Figure 1 Mapping of specific domains of merlin responsible for the association with RalGDS. **(a)** Schematic diagram of the merlin and RalGDS constructs used in the yeast two-hybrid assays. The merlin proteins were fused with GAL4-DBD, and RalGDS proteins were fused with GAL4-AD. **(b)** A summary of the yeast two-hybrid results using RalGDS and merlin proteins. The plasmids were co-transformed into the yeast cells and the binding ability was tested. The β-galactosidase assay (lacZ activity) and the growth of yeast cells in the absence of histidine were performed as described in Materials and methods. The growth abilities of the His^+ colonies are indicated as either (+) or (−)

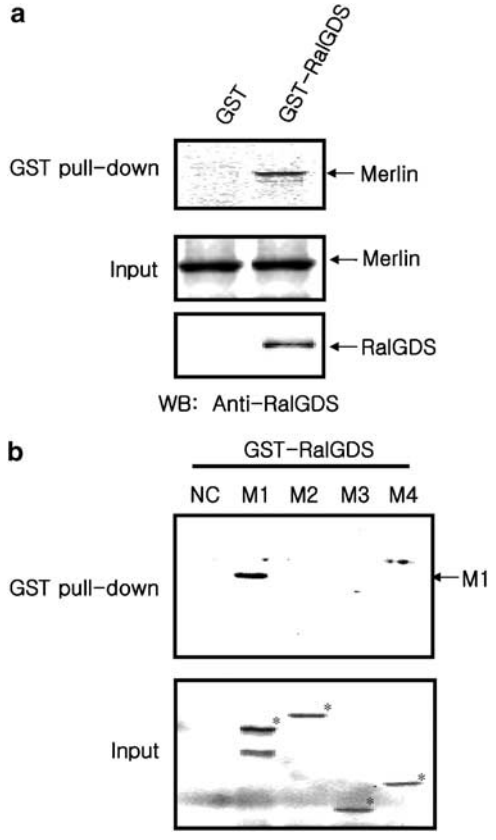

Figure 2 *In vitro* interaction of RalGDS and merlin. **(a)** The GST pull-down assay with RalGDS and merlin. Merlin protein was labeled with [^{35}S]methionine by *in vitro* translation and incubated with 2 μg of GST or GST-RalGDS protein for 2 h at 4°C. After extensive washing, the bound merlin was extracted and detected with PhosphorImager (upper panel). The amount of added merlin in the reticulocyte lysate is shown in the middle panel. The GST–RalGDS fusion proteins were subjected to SDS–polyacrylamide gel electrophoresis and subsequent Western blotting analysis using the anti-RalGDS antibody (bottom panel). **(b)** The binding of the deletion mutants of merlin with RalGDS. Each mutant protein was labeled with [^{35}S]methionine by *in vitro* translation and incubated with 2 μg of the resin-bound GST-RalGDS for 2 h at 4°C. Washing and detection of merlin proteins were performed as described above using PhosphorImager (upper panel). The amount of merlin mutants in each reticulocyte lysate is shown in the lower panel. The asterisks indicate the positions of merlin mutants expected from their calculated molecular weight. WB: Western blotting

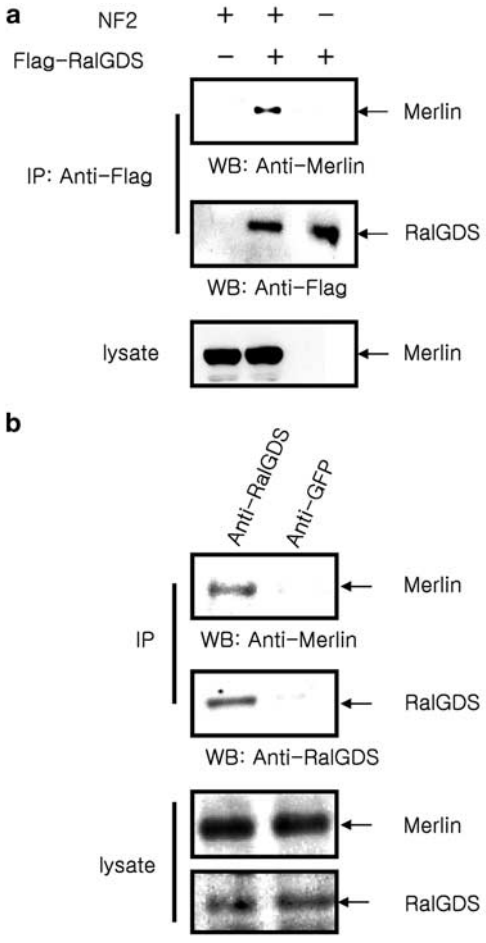

Figure 3 Association of RalGDS and merlin in NIH3T3 cells. **(a)** NIH3T3 cells were transfected with 1.2 μg of the merlin expression plasmid with or without the expression plasmid for Flag-tagged RalGDS as indicated. The cell lysates were subjected to immunoprecipitation with the anti-Flag antibody and immunoblotting with the anti-merlin antibody (top panel). The level of the immunoprecipitated Flag-RalGDS was analysed by Western blot using the anti-Flag antibody (middle panel). The amount of the added merlin in each lysate is shown in the bottom panel. **(b)** The interaction of merlin with RalGDS at the endogenous level. The cell lysates were immunoprecipitated with anti-RalGDS or anti-GFP antibody, and immunoblotted with the anti-merlin antibody (top panel). The level of the immunoprecipitated RalGDS was analysed by Western blotting with the anti-RalGDS antibody (middle panel). The endogenous level of merlin and RalGDS in each lysate is shown in the two bottom panels. WB: Western blotting, IP: immunoprecipitation

between the M3 or M4 merlin mutant and RalGDS was too weak to be detected in the *in vitro* binding assay and the β-galactosidase assay in yeast.

In order to further demonstrate the interaction between RalGDS and merlin in animal cells, NIH3T3 cells were co-transfected with the plasmids expressing Flag-tagged RalGDS and merlin. The cell lysates were subjected to immunoprecipitation with anti-Flag antibody. Subsequent Western blotting with the anti-merlin antibody revealed that merlin interacted with RalGDS in NIH3T3 cells (Figure 3a). Then, we examined whether endogenous merlin and RalGDS interact in intact cells. When assessed by co-immunoprecipitation in NIH3T3 cells, endogenous merlin was observed only in the RalGDS immune complex but not in the control GFP immune complex (Figure 3b). Overall, these results indicate that RalGDS interacts with merlin in intact cells at the endogenous level.

RalGDS co-localizes with merlin in vivo

Merlin is known to present primarily in the cytoplasmic membrane (Chishti *et al*., 1998) and is also found around the membrane-ruffling region and in granules/vesicles at the perinuclear region (Schmucker *et al*., 1999). In order to determine if RalGDS co-localizes with

merlin, they were co-expressed in NIH3T3 cells and immunostained with the specific antibodies. The fluorescence images were analysed by confocal microscopy. When expressed separately, merlin was mainly detected at the cytoplasmic membrane and the perinuclear region (Figure 4a) as expected, while RalGDS was distributed throughout the cytoplasm (Figure 4d). When they were co-expressed, the perinuclear merlin was decreased and RalGDS appeared to be enriched at the cytoplasmic membrane, where they were mainly co-localized (Figure 4e–g). The co-localization of merlin and RalGDS was also observed at the endogenous level in NIH3T3 cells without the overexpression of these proteins (Figure 4n–p). To correlate the result with that of the domain analysis, we perform the experiment with the M1 and M2 merlin mutants. The M1 merlin mutant showed a cellular localization pattern similar to the wild-type merlin, but was enriched at the perinuclear region (Figure 4b). However, the M2 merlin mutant was mainly detected at the nucleus with some cytoplasmic localization, which was not normally observed with the wild-type merlin (Figure 4c). When co-expressed with the M1 or M2 mutants, RalGDS was co-localized with the M1 mutant (Figure 4h–j) but not with the M2 mutant (Figure 4k–m), as expected from their *in vitro* interaction result. Overall, these results suggest that both the overexpressed and endogenous merlin are co-localized with RalGDS in animal cells.

Merlin inhibits the RalGDS activity

RalGDS is one of the Ras effectors and stimulates the GDP/GTP exchange of Ral, which is a member of the Ras superfamily of GTPases that cycles between the active GTP-bound and inactive GDP-bound states (Feig *et al*., 1996). Indeed, RalGDS promotes the release of GDP from Ral and GTP binding in its place, which activates Ral. The active GTP-bound Ral can specifically interact with a distinct set of downstream target proteins such as RalBP1 (or RLIP) and POB1 (Cantor *et al*., 1995; Yamaguchi *et al*., 1997; Ikeda *et al*., 1998).

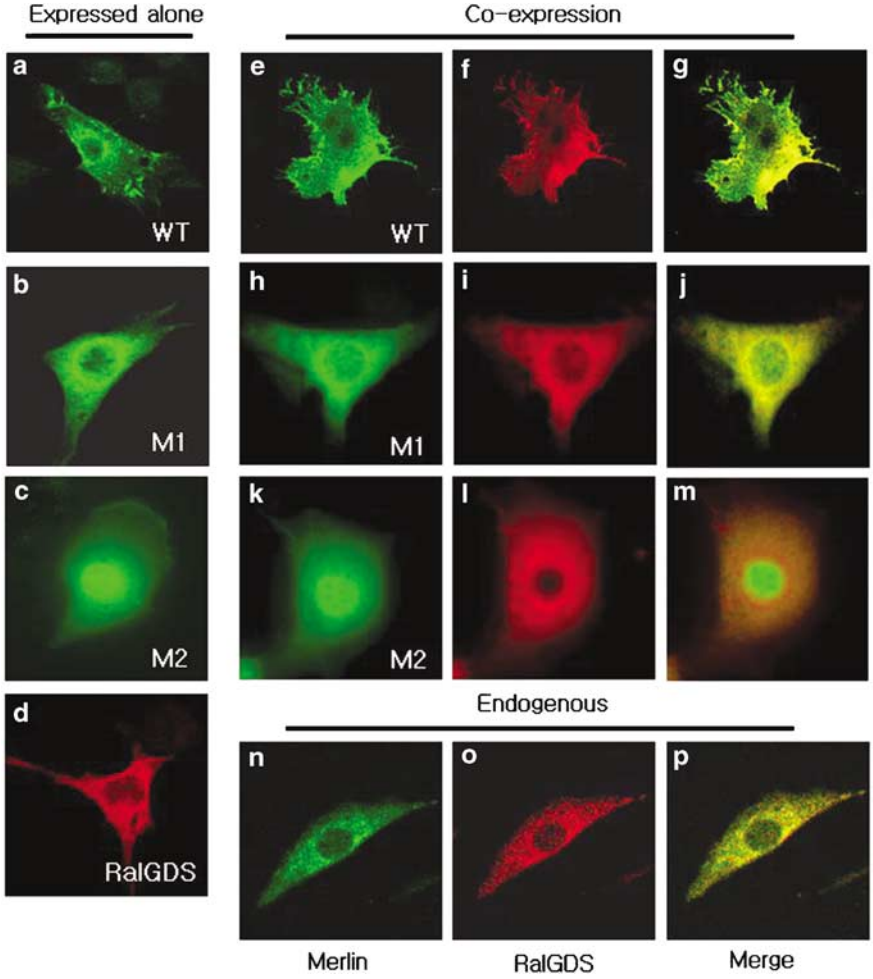

Figure 4 Co-localization of merlin with RalGDS in NIH3T3 cells**.** NIH3T3 cells were grown on the chamber slides and transfected with pcDNA-NF2, pcDNA3.1-M1, pcDNA3.1-M2 and/or pcDNA3.1-RalGDS as indicated. The cells were fixed, permeabilized and stained with anti-merlin **(a–c, e, h** and **k)** or anti-RalGDS **(d, f, i** and **l)** antibodies. The endogenous merlin and RalGDS were also stained with anti-merlin (n) or anti-RalGDS (o) antibodies. The fluorescence images were captured using confocal microscopy. The co-localization of merlin and RalGDS is shown by the yellow color in the overlay image **(g, j, m** and **p)**

In order to investigate the functional significance of their interaction, the effect of merlin on the RalGDS-mediated activation of RalA was assessed via the binding activity of RalA to the Ral-binding domain of RalBP1. RalGDS and RalA were transiently expressed in Nf2-deficient or wild-type mouse embryo fibroblasts (MEFs) in combination with the full-length or deletion mutants of merlin, and the RalGDS activity was measured indirectly by the level of the GTP-bound active RalA protein in the pull-down complex of RalBP1.

As shown in Figure 5a, RalGDS induced the association between RalBP1 and RalA both in the $Nf2^{-/-}$ and $Nf2^{+/+}$ MEFs, but with the level of active RalA somewhat higher in $Nf2^{-/-}$ MEF than in $Nf2^{+/+}$ MEFs. Co-expression of the full length or M1 mutant of merlin, but not of the M2 mutant, in $Nf2^{-/-}$ MEFs inhibited their interaction, which indicates that exogenous merlin reduces RalGDS-mediated activation of RalA. The levels of the overexpressed proteins and β-actin in the transfected cells were monitored by Western blotting (Figure 5a, four bottom panels). These results suggest that the interaction between merlin and RalGDS leads to the inhibition of RalA activation. The effect of merlin on the RalGDS-mediated activation of RalA was also observed in NIH3T3 cells (data not shown).

The effect of merlin on the RalGDS activity was also analysed by measuring the ratio of GTP over the total guanine nucleotides bound to RalA. COS7 cells were transfected with the expression plasmids as above, and labeled with [^{32}P]orthophosphate. After immunoprecipitation with the anti-RalA antibody, the radiolabeled GTP and GDP were separated by TLC and quantified using a PhosphoImager. When co-expressed with RalA, RalGDS induced significantly the RalA-bound GTP content in COS7 cells (Figure 5b). However, the additional expression of merlin inhibited this RalGDS activity. The EGF treatment was used as a positive control for RalA activation. These results strongly suggest that merlin can directly inhibit the ability of RalGDS to activate RalA.

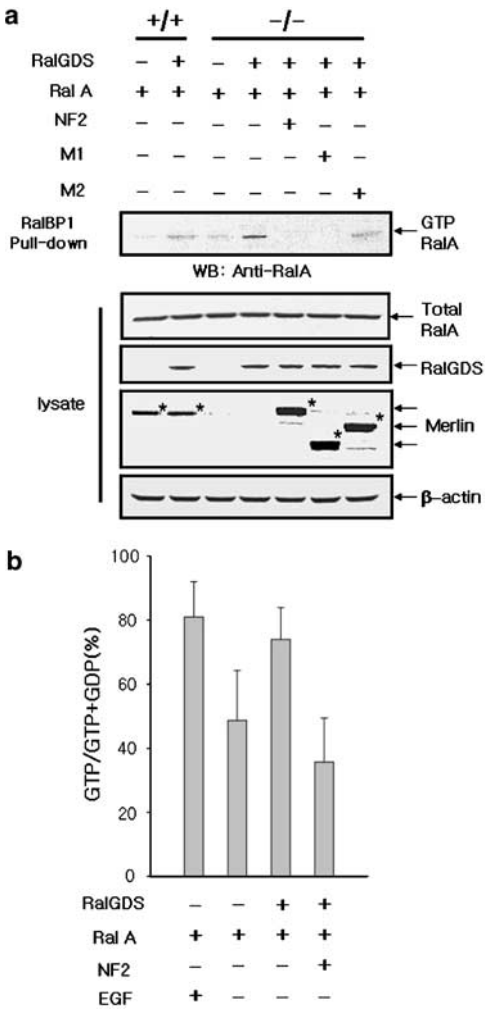

Figure 5 Effect of merlin on the RalGDS activity. **(a)** $Nf2^{-/-}$ and $Nf2^{+/+}$ MEFs (2×10^5) were transfected with 1 μg each of RalA, RalGDS and/or expression vectors for the full-length merlin, the M1 and M2 mutants of merlin as indicated. The GTP-bound RalA was quantified after precipitation with the resin-bound RalBP1. The level of the active RalA was analysed with the RalA antibody (pull-down). The cell lysates were subjected to Western blotting in order to control the cellular levels of RalA, RalGDS, merlin and β-actin (lysate). The asterisks indicate the positions of merlin and its mutants (M1 and M2) expected from their calculated molecular weight. **(b)** COS7 cells (3×10^5) were transfected with 1 μg each of RalA, RalGDS and/or merlin expression vectors as indicated, and labeled with [^{32}P]orthophosphate for 4 h. After the immunoprecipitation of RalA, the bound guanidine nucleotides were eluted and separated on TLC. The intensity of the GDP and GTP spots was quantified and the GTP/(GTP + GDP) ratio was calculated. The experiments were performed three times in duplicate and the results were averaged. The standard errors are shown on the top of each bar

Merlin inhibits the colony formation of NIH3T3 cells by RalGDS and RalA

Similar to the active Ras(12V, 37G), RalGDS induces the formation of foci and growth of morphologically transformed NIH3T3 cells in the presence of active Raf (McCormick and Wittinghofer, 1996). Moreover, Ral protein is involved in the Ras-dependent transformation of NIH3T3 cells (Vojtk and Der, 1998; Wolthuis *et al*., 1998; Joffe and Adam, 2001). Accordingly, the effect of merlin on the cellular functions of RalGDS was investigated by a colony formation assay. NIH3T3 cells were co-transfected with the expression vectors for RalGDS and RalA in the presence or absence of merlin and its deletion mutants (M1 and M2 mutants). The pcDNA3.1 plasmid was used as the negative control. The cells were selected with G418 for 2 weeks and the number of colonies formed on the plates was counted. As shown in Figure 6b, the number of G418-resistant colonies in the presence of RalGDS and RalA was about three times higher than the control. However, the number of colonies was significantly lower when either the wild-type merlin or M1 mutant was co-expressed with them. The M2 deletion mutant of merlin showed no effect on the colony formation by RalGDS and RalA. The expression of RalA or RalGDS alone was not efficient in inducing a colony transformation of

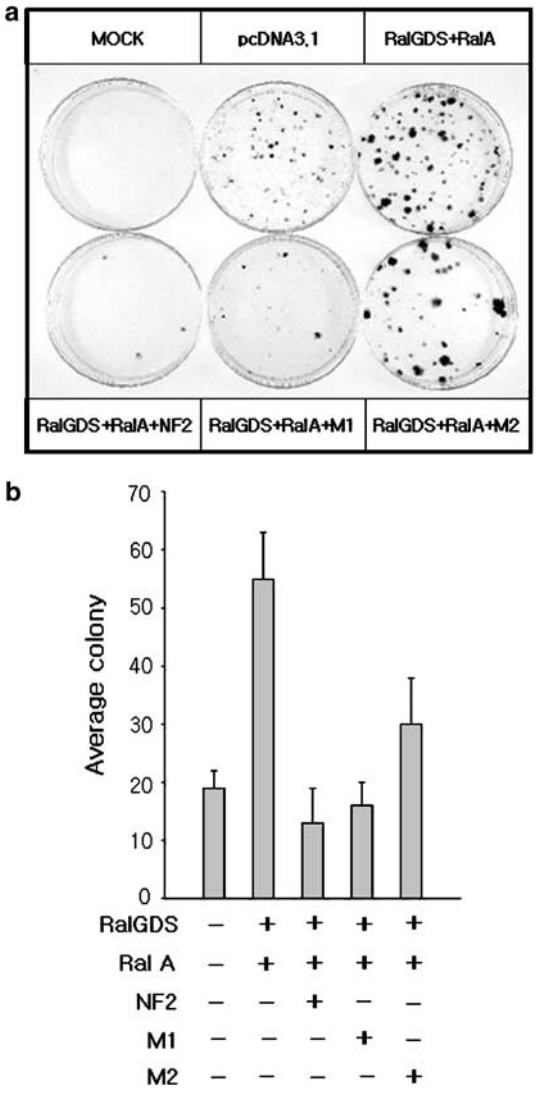

Figure 6 Inhibition of RalGDS and RalA induced colony formation of NIH3T3 cells by merlin. **(a)** NIH3T3 cells (3×10^5) were transfected with 1.2 μg each of pcDNA-Flag-RalGDS, pcDNA3-HA-RalA and/or pcDNA-NF2, pcDNA-M1 and pcDNA-M2 as indicated. NIH3T3 cells nontransfected or transfected with pcDNA 3.1 were used as the negative controls. The cells were selected for 2 weeks with 400 μg/ml G418. The experiments were performed three times and a representative image was taken. **(b)** The number of colony formed in **(a)** was counted and the results were averaged. The standard errors are shown on the top of each bar

NIH3T3 cells (data not shown) as reported (White *et al*., 1996). The representative plate images are shown in Figure 6a. These results suggest that merlin suppresses the RalGDS and RalA-mediated cell growth.

Merlin inhibits the RalGDS-induced cell migration

The activation of the Ras–Ral pathway by the active form of Ras, RalGDS or Ral is shown to increase the motility of myoblast (Suzuki *et al*., 2000). Therefore, we investigated whether the activation of RalGDS stimulates the migration of NIH3T3 cells and merlin inhibits the stimulatory effect of RalGDS. The NIH3T3 cell lines expressing the control plasmid or RalGDS were constructed for this experiment. A wound-healing assay was performed as described in Materials and methods in the presence of EGF to induce cell migration (Melchiori *et al*., 1990; Gildea *et al*., 2002; Takaya *et al*., 2004). Mitomycin C was treated to the cells in order to avoid the confounding effect of cell proliferation. The control and RalGDS stable cells were infected with the adenovirus expressing GFP (Ad-GFP) or merlin (Ad-NF2) with the EGF treatment. As shown in Figure 7a, the RalGDS stable cells migrated to the wound front approximately three times faster than the control cells. However, this migration was reduced approximately by the half when the cells were infected with Ad-NF2. An infection of Ad-GFP showed no effect on the wound healing of both the control and RalGDS stable cells (data not shown). The effect of merlin and RalGDS on the motility of NIH3T3 cells was also examined in a modified Boyden chamber assay (see Materials and methods for details). The control and RalGDS stable cells were infected with an adenovirus expressing either GFP (Ad-GFP) or merlin (Ad-NF2) with or without the EGF treatment. When infected with the Ad-GFP, the RalGDS stable cells migrated faster than the control cells both in the presence or absence of EGF (Figure 7b). In contrast, the RalGDS stable cells showed a reduced motility by a Ad-NF2 infection regardless of the EGF treatment, the level of which was even lower than that of the Ad-GFP-infected cells. Overall, these results suggest that RalGDS enhances the motility of NIH3T3 cells and merlin can abolish the RalGDS-induced cell migration.

Discussion

In this study, we identified RalGDS as a merlin-binding protein by yeast two-hybrid screening (Figure 1). The *in vitro* and *in vivo* binding experiments showed that RalGDS and merlin interact directly, even at the endogenous level (Figures 2–4), suggesting the biological relevance of their interaction under physiological conditions.

RalGDS is known as one of Ras effector proteins and functions as a guanine-nucleotide exchange factor for Ral protein, stimulating the dissociation of GDP from and the binding of GTP to Ral. We showed that merlin inhibits the ability of RalGDS activating RalA, which suggests that merlin might negatively regulate the RalGDS-mediated signaling pathways (Figure 5).

The biological significance of their interaction was also shown in the colony formation assay in NIH3T3 cells. It was reported that the RalGDS–Ral signaling pathway is involved in the Ras-dependent outgrowth of NIH3T3 cells (White *et al*., 1996). In this study, the overexpression of merlin inhibited the RalGDS and RalA-induced colony formation of NIH3T3 cells (Figure 6). This suggests that merlin can suppress the

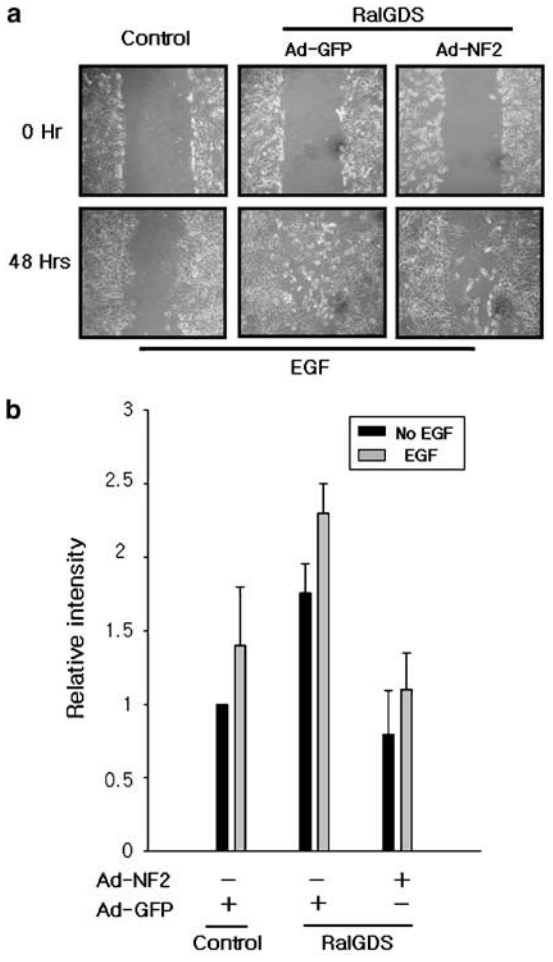

Figure 7 Suppression of RalGDS-induced cell migration of NIH3T3 cells by merlin. **(a)** Monolayers of the stable NIH3T3 cells (2×10^5) expressing pcDNA3.1 (control) or RalGDS were infected with 100 moi each of Ad-GFP or Ad-NF2 and treated with EGF and wounded with a pipette tip. The healing of the wound fronts was examined after 48 h using phase contrast microscopy. A representative image of three independent experiments is shown. **(b)** The control and the RalGDS stable NIH3T3 cells (3×10^5) were plated on the chamber slides and infected with 100 moi each of Ad-GFP or Ad-NF2 as indicated. The cells in the upper chamber were cultured in serum-free DMEM, and the lower chamber was filled with DMEM containing 10% FBS. After 6 h, the cells were lysed and stained with a CyQuant GR dye. The migration of cells was quantified by the fluorescence intensities. The experiments were performed three times in duplicate and the results were averaged. The standard errors are shown on the top of each bar

RalGDS and RalA-mediated cell growth, which is in agreement with the previous reports (Shermn *et al*., 1997; Ikeda *et al*., 1999; Morrison *et al*., 2001). In addition to suppressing cell growth, the overexpression of merlin was reported to reverse the HA-ras-induced malignant phenotypes of NIH3T3 cells and restore the contact inhibition of the cell (Tikoo *et al*., 1994). Many studies have shown that merlin inhibits the diverse Ras-mediated signaling pathways (Kim H *et al*., 2002; Lim *et al*., 2003; Hirokawa *et al*., 2004), but no direct target of merlin has been identified. We suggest here that inhibition of RalGDS activity via direct interaction can be one of the mechanisms by which merlin suppresses the Ras-signaling pathways.

Ral is known to regulate myoblast cell migration and the initiation of border cell migration during Drosophila oogenesis (Lee *et al*., 1996; Suzuki *et al*., 2000). In contrast, the effect of RalGDS on the cell migration has not been reported. We showed here that the overexpression of RalGDS enhanced the motility of NIH3T3 cells and co-expression of merlin inhibited the RalGDS-induced cell migration (Figure 7). The migration ability of cells is thought to be associated with the metastatic potential of tumors (Arvelo and Poupon, 2001). The inhibition of the RalGDS signaling pathways by a dominant-negative Ral protein blocks Ras-mediated metastatic growth of cells (Urano *et al*., 1996; Lu *et al*., 2000). In addition, the germ line heterozygous *NF2* mutant mice develops a variety of aggressive malignancies noticeably with the metastatic property (McClatchey *et al*., 1998). Therefore, the inhibition of Ral activity by merlin via the interaction with RalGDS might contribute to the antimetastatic activity of merlin.

Currently, the mechanism for how merlin inhibits the RalGDS activity is unclear. Merlin has no known enzymatic activities and is believed to modulate various protein–protein interactions depending on its folding state (Scoles *et al*., 2002). Therefore, it is most plausible that merlin inhibits RalGDS activity by interfering directly with the interaction of RalGDS with other signaling proteins. The domain analysis showed that merlin interacts with the C-terminal RBD of RalGDS (Figures 1 and 2). This suggests that merlin might interfere with the interaction between Ras and RalGDS. However, there might be additional regulation mechanisms, because merlin inhibited the activity of the overexpressed RalGDS without stimulating signals from Ras (Figures 5–7). In merlin, the region containing the 'Blue Box' (BB) sequence of FERM domain (aa 131–201) is involved in the interaction with RalGDS (Figures 1 and 2). Despite merlin sharing a high sequence homology with the ERM proteins in the FERM domain, this seven-residue BB (aa 177–183, YQMTPEM) was not conserved in the ERM proteins (Sun *et al*., 2002). Therefore, this BB sequence might be responsible for the unique function of merlin as tumor suppressor and its interaction with a distinct set of proteins including RalGDS. Interestingly, we observed that the M2 merlin mutant that lacks the BB-containing region was localized mainly in the nucleus where the wild-type melin is not normally detected (Figure 4). This suggests that the BB could be involved in the nuclear/cytoplasmic shuttling of merlin as previously suggested (Johnson *et al*., 2002; Kressel and Schmucker, 2002).

In conclusion, this report demonstrates that RalGDS is a novel binding partner of merlin, and suggests that their interaction might provide one of the important pathways regulating the oncogenic transformation and the migration of cells. However, the detailed mechanism underlying their interaction requires further investigations to be elucidated.

Materials and methods

Plasmids

The yeast plasmids for the wild-type (WT) merlin and its deletion mutants (M1–M4) were generated by cloning the PCR fragments into pGBT9, a GAL4 DNA-binding domain vector (Clontech, Palo Alto, CA, USA). The *Bam*HI restriction sites were used for both the 5′- and 3′-ends. The plasmids encoding the C-terminal or the full length of human RalGDS were also generated by PCR cloning into pACT2, a GAL4 activation domain vector (Clontech, Palo Alto, CA, USA), using *Eco*RI (5′ primers) and *Xho*I (3′ primers) restriction sites. The mammalian expression plasmids for the WT merlin and its deletion mutants (M1–M4) were described previously (Kim JY *et al*., 2002). The mammalian expression plasmid for the wild-type RalGDS (pcDNA-Flag-RalGDS) was constructed by inserting the PCR fragment into the *Eco*RI–*Hin*dIII sites of pcDNA3.1-Flag (Invitrogen, San Diego, CA, USA). A Flag epitope was tagged at the N-terminal end of RalGDS. The GST-fusion construct of the wild-type RalGDS (pGEX-KG-RalGDS) was also generated by PCR and subcloned into pGEX-KG (Pharmacia, Piscataway, NJ, USA) using *Eco*RI–*Hin*dIII sites. The mammalian expression plasmid of RalA (pcDNA3-HA-RalA) was a kind gift from Dr Takashi Iwamoto.

Yeast two-hybrid screening

A cDNA encoding the full-length human merlin was used as bait in the yeast two-hybrid screens of a human brain cDNA library in pACT2 (Clontech, Palo Alto, CA, USA). The bait and the library DNAs were co-transformed to yeast using the lithium acetate method as described previously (Gietz *et al*., 1992). The transformants were selected for growth on the Leu^-, Trp^-, His^- and Ade^- solid media containing 25 mM 3-aminotriazole (3-AT). The β-galactosidase production was assayed by incubating freeze-fractured colonies on nitrocellulose in a Z-buffer (60 mM Na_2HPO_4, 40 mM NaH_2PO_4, 10 mM KCl, 1 mM $MgSO_4$, 0.03 mM β-mercaptoethanol and 2.5 μM X-gal) at 30°C.

cDNA cloning

The full-length cDNA encoding RalGDS was cloned using the Marathon cDNA Amplification system (Clontech, Palo Alto, CA, USA). Briefly, 5′-RACE was performed using the human placenta cDNA template. The PCR condition was as follows: 94°C for 1 min; five cycles of 94°C for 30 s, 72°C for 3 min; five cycles of 94°C for 30 s, 70°C for 30 s, 72°C for 3 min; and 25 cycles of 94°C for 30 s, 68°C for 30 s, 72°C for 3 min. From the experiment, a ~2.7 kb cDNA was obtained and cloned in the TOPO TA Cloning vector (Invitrogen Corp, Carlsbad, NM, USA) and the sequence was verified.

Construction of stable cell lines

NIH3T3 cells were obtained from the American Type Culture Collection (Manassas, VA, USA) and maintained in DMEM supplemented with 10% FBS and antibiotics. In order to construct a stable cell line, NIH3T3 cells were transfected with pcDNA-Flag-RalGDS or pcDNA3.1 plasmid as a control. After 48 h, the cells were split at a 10 : 1 ratio and cultured in the medium containing 400 μg/ml G418 for 3 weeks. The individual G418-resistant colonies were isolated and the overexpressed RalGDS was confirmed by Western blotting.

Transient transfection

NIH3T3 (3×10^5 cells) were plated on a 35 mm plate and transfected with the plasmids using Gene Porter2 reagent according to the manufacturer's instruction (Gene Therapy System Inc.). The total amount of the transfected DNA was normalized using the pcDNA3.1 plasmid as a carrier.

GST pull-down assay

The GST fusion protein encompassing the full-length RalGDS was expressed in *Escherichia coli* and purified as described previously (Hofer *et al*., 1994). *In vitro* translation was performed to obtain wild-type merlin and its deletion mutants labeled with [^{35}S]methionine using the TNT T7 Coupled Reticulocyte Lysate System (Promega, Madison, WI, USA). For the pull-down assay, 2 μg of GST-RalGDS was immobilized on the glutathione-Sepharose 4B beads and incubated with the ^{35}S-labeled merlin proteins in RIPA-B buffer (0.5% Nonidet P-40, 20 mM Tris (pH 8.0), 50 mM NaCl, 50 mM NaF, 100 μM Na_3VO_4, 1 mM DTT and 50 μg/ml PMSF) for 2 h at 4°C. After washing with the RIPA-B buffer, the samples were analysed by SDS–PAGE and a PhosphorImager.

Immunoprecipitation

The anti-merlin, anti-RalGDS (Santa Cruz Biotechnology, Inc.) and anti-Flag (Sigma, Inc.) antibodies were obtained from commercial sources. For immunoprecipitation, NIH3T3 cells (3×10^5 cells) in 35-mm plate were transfected with 1.0 μg each of the expression plasmids as indicated in Figure 3a. After 24 h, the cells were lysed in the RIPA-B buffer for 20 min on ice. The insoluble material was removed by centrifugation at 12 000 rpm for 20 min at 4°C. The supernatant was incubated with the anti-Flag antibodies for 5 h at 4°C, and then incubated for 2 h with the pre-cleared protein A agarose bead (Sigma, Inc). Subsequently, the beads were washed three times in RIPA buffer and re-suspended in 50 μl of 1 × SDS sample buffer. The samples were analysed by Western blotting using the anti-merlin antibody.

Immunocytochemistry

NIH3T3 cells (7×10^4) in a chamber slide (NUNC, four well) were transfected with 1.0 μg each of the expression plasmids as indicated in Figure 4. After 24 h, the cells were rinsed with 1 × PBS and fixed with 4% paraformaldehyde for 20 min. Then, the cells were permeabilized in PBS containing 0.5% Triton X-100 for 15 min and the slides were blocked with 0.2% BSA in PBS for 30 min. The chamber slides were incubated with anti-merlin (1 : 500) and anti-RalGDS (1 : 100) antibodies overnight at 4°C, and rinsed with PBS five times. The FITC-conjugated anti-rabbit and the rhodamine-conjugated anti-goat secondary antibodies (Santa Cruz Biotechnology, Inc.) were used for anti-merlin and anti-RalGDS antibodies, respectively. The chamber slides were mounted on glass slides and the images were acquired using confocal laser-scanning microscopy.

Ral activity assay in mammalian cells

$Nf2^{-/-}$ and $Nf2^{+/+}$ MEFs (2×10^5 cells) in the 35-mm plate were transfected with 1.0 μg each of the expression plasmids as indicated in Figure 5a. After 24 h, the cells were lysed with lysis buffer (1% Triton, 20 mM Tris-HCl (pH 7.5), 10 mM $MgCl_2$, 150 mM NaCl, 1 mM PMSF, 1 mM Na_3VO_4, 50 mM NaF, 10 μg/ml leupeptin and 10 μg/ml aprotinin) for 20 min on ice. The cell lysates were incubated with 2 μg of GST-fused RBD of RalBP1 (GST-RalBP1, Upstate Biotechnology, Inc.) for 1 h at

4°C. Then, the beads were precipitated by centrifugation, extensively washed and analysed by Western blotting using the anti-RalA antibody (Upstate Biotechnology, Inc.). The principle for assessing the RalA activation is described in the Results section.

GDP/GTP exchange assay of RalGDS in mammalian cells

COS7 cells (3×10^5 cells) in 35-mm plate were transfected with 1.0 μg each of the expression plasmids as indicated in Figure 5b. After 24 h, the cells were starved in DMEM with 1.5% FBS for 16 h, washed with serum-free media and incubated in the phosphate-free media containing 0.3 mCi of [^{32}P]orthophosphate for 5 h. The cell lysates were prepared as described above. RalA protein was immunoprecipitated with the anti-RalA antibody and washed extensively with washing buffer (20 mM Tris-HCl (pH 7.5) and 10 mM $MgCl_2$). The radio-labeled GTP/GDPs were eluted with an elution buffer (0.2% SDS, 5 mM EDTA, 5 mM GDP and 5 mM GTP) and separated by thin-layer chromatography (TLC) on polyethylenimin-cellulose (Sigma, Inc.). The signals were autoradiographed, and the GTP/(GDP + GTP) ratio was determined using the PhosphorImager and ImageQuant software.

Colony formation assay

NIH3T3 cells (3×10^5 cells) on the 35-mm plate were transfected with 1.0 μg each of the expression plasmids as indicated in Figure 6. After 48 h, the cells were split at a 2 : 1 ratio and the G418-resistant colonies were selected with 400 μg/ml G418 for 2 weeks. The cells were fixed in PBS containing 0.2% glutaraldehyde and 0.5% formaldehyde for 10 min on ice and stained with 0.2% crystal violet for 10 min at room temperature. The average number of colonies was determined from the experiments performed three times in duplicate.

Adenovirus production and infection

The adenovirus expressing merlin (Ad-NF2) was kindly provided by Dr SS Jeun (Catholic University of Korea), and the adenovirus expressing green fluorescent protein (Ad-GFP) was purchased from Neurogenex Co., Ltd (Seoul, Korea). Viruses were propagated in HEK293, a human embryonic kidney cell line. In order to purify the viruses, freezing/thawing of cells and subsequent centrifugation were peformed. The viral titer was determined by limiting-dilution bioassay in HEK293 cells as described previously (Matthews, 2002). The infection was performed for 2 h at a concentration of 100 moi/well (35-mm plates).

Cell migration assay

The cell migration assay was performed using two methods: the wound-healing assay and the modified Boyden chamber assay. For the wound-healing assay, the control and RalGDS stable cells were plated at a density of 2×10^5 cells in a 35-mm plate and infected with 100 moi each of the adenoviruses. After 12 h, the cell monolayer was wounded with a pipette tip by approximately 1 mm in width. Then the cells was removed of debris by washing twice with PBS and cultured at 37°C in DMEM containing 0.1 μg/ml mitomycin C and 20 ng/ml EGF. After 48 h, the migration of the cells at the wound front was photographed using an inverted microscope.

For the modified Boyden chamber assay (96 well, 8-μm pores, Chemicon, Inc.), the control and RalGDS stable cells were plated at a density of 3×10^5 cells in a 35-mm plate and infected with 100 moi each of the adenoviruses. After 12 h, the stable cells were starved in DMEM containing 1.5% FBS for 16 h, trypsinized and re-suspended at a density of 2×10^5 cells/ml in serum-free DMEM in the presence or absence of 20 ng/ml EGF. The cell suspension was plated onto the upper chamber and DMEM containing 10% FBS was placed in the lower chamber. The chamber culture was incubated for 6 h at 37°C and, then, the nonmigrated cells were washed off the upper surface of the membrane. The migrated cells on the bottom side were dissociated with Cell Detachment Buffer (Chemicon, Inc.), lysed and stained for nucleic acids with CyQuant GR dye (Molecular Probes). The signal intensities were measured using a fluorescence reader (HIDEX, Inc.). The result was presented as the average values from three independent experiments performed in duplicates.

Acknowledgements
We wish to thank other members of the laboratory for their assistance. We also thank Dr David Gutmann and Dr Takashi Iwamoto for providing us pcDNA-NF2 and pcDNA3-RalA expression vector, respectively. This study was supported by a grant of the Korean Health 21 R&D Project, Ministry of Health and Welfare, Republic of Korea (00-PJ3-PG6-GN02-0002, 02-PJ10-PG6-GN01-0002).

References

Arvelo F and Poupon MF. (2001). *Acta Cient Venez.*, **52,** 304–312.
Cantor S, Urano T and Feig LA. (1995). *Mol. Cell. Biol.*, **15,** 4578–4584.
Chishti AH, Kim AC, Marfatia SM, Lutchman M, Hanspal M, Jindal H, Liu SC, Low PS, Rouleau GA, Mohandas N, Chasis JA, Conboy JG, Gascard P, Takakuwa Y, Huang SC, Benz Jr EJ, Bretscher A, Fehon RG, Gusella JF, Ramesh V, Solomon F, Marchesi VT, Tsukita S, Tsukita S, Arpin M, Louard D, Tonks NK, Anderson JM, Fanning AS, Bryant PJ, Woods DF and Hoover KB. (1998). *Trends Biochem. Sci.*, **23,** 281–282.
Feig LA, Urano T and Cantor S. (1996). *Trends Biochem. Sci.*, **21,** 438–441.
Fernandez-Valle C, Tang Y, Ricard J, Rodenas-Ruano A, Taylor A, Hackler E, Biggerstaff J and Iacvelli J. (2002). *Nat. Genet.*, **31,** 354–362.
Gietz D, St. Jean A, Woods RA and Schiestl RH. (1992). *Nucleic Acids Res.*, **20,** 1425.
Gildea JJ, Harding MA, Seraj MJ, Gulding KM and Theodorescu D. (2002). *Cancer Res.*, **62,** 982–985.
Goutebroze L, Brault E, Muchardt C, Camonis J and Thomas G. (2000). *Mol. Cell. Biol.*, **20,** 1699–1712.
Hirokawa Y, Tikoo A, Huynh J, Utermark T, Hanemann CO, Giovannini M, Xiao GH, Testa JR, Wood J and Maruta H. (2004). *Cancer J.*, **10,** 20–26.
Hofer F, Fields S, Schneider C and Martin GS. (1994). *Proc. Natl. Acad. Sci. USA*, **91,** 11089–11093.
Ikeda M, Ishida O, Hinoi T, Kishida S and Kikuchi A. (1998). *J. Biol. Chem.*, **273,** 814–821.
Ikeda K, Saeki Y, Gonzalez-Agosti C, Ramesh V and Chiocca EA. (1999). *J. Neurosurg.*, **91,** 85–92.
Jannatipur M, Dion P, Khan S, Jindal H, Fan X, Laganiere J, Chishti AH and Rouleau GA. (2001). *J. Biol. Chem.*, **276,** 33093–33100.
Joffe EB and Adam A. (2001). *Medicina*, **61,** 658–663.
Johnson KC, Kissil JL, Fry JL and Jacks T. (2002). *Oncogene*, **21,** 5990–5997.

Joneson T and Bar-Sagi D. (1997). *J. Mol. Med.*, **75,** 539–587.
Kim H, Lim JY, Kim YH, Kim H, Park SH, Lee KH, Han H, Jeun SS, Lee JH and Rha HK. (2002). *Mol. Cells*, **14,** 108–114.
Kim JY, Kim H, Jeun SS, Rha SJ, Kim YH, Ko YJ, Won J, Lee KH, Rha HK and Wang YP. (2002). *Biochem. Biophys. Res. Commun.*, **296,** 1295–1302.
Koga H, Araki N, Takeshia H, Nishi T, Hirota T, Kimura Y, Nakao M and Saya H. (1998). *Oncogene*, **17,** 801–810.
Kressel M and Schmucker B. (2002). *Hum. Mol. Genet.*, **11,** 2269–2278.
Lee IK, Kim KS, Kim H, Lee JY, Ryu CH, Chun HJ, Lee KU, Lim Y, Kim YH, Huh PW, Lee KH, Han SI, Jun TY and Rha HK. (2004). *Biochem. Biophys. Res. Commun.*, **325,** 774–783.
Lee JY, Kim H, Ryu CH, Kim JY, Choi BH, Lim Y, Huh PW, Kim YH, Lee KH, Jun TY, Rha HK, Kang JK and Choi CR. (2004). *J. Biol. Chem.*, **279,** 30265–30273.
Lee T, Feig L and Montell DJ. (1996). *Development*, **122,** 409–418.
Lim JY, Kim H, Kim YH, Kim SW, Huh PW, Lee KH, Jeun SS, Rha H and Kand Kang JK. (2003). *Biochem. Biophys. Res. Commun.*, **302,** 238–245.
Louis DN, Ramesh V and Gusella JF. (1995). *Brain Pathol.*, **5,** 163–172.
Lu Z, Hornia A, Joseph T, Sukezane T, Frankel P, Zhong M, Bychenok S, Xu L, Feig LA and Foster DA. (2000). *Mol. Cell. Biol.*, **20,** 462–467.
Matthews JN. (2002). *Dev. Biol.*, **107,** 87–94.
McClatchey AI, Saotome I, Mercer K, Crowley D, Gusella JF, Bronson RT and Jacks T. (1998). *Genes Dev.*, **12,** 1121–1133.
McCormick F and Wittinghofer A. (1996). *Curr. Opin. Biotechnol.*, **7,** 449–456.
Melchiori A, Carlone S, Allavena G, Aresu O, Parodi S, Aaronson SA and Albini A. (1990). *Anticancer Res.*, **10,** 37–44.
Morrison H, Sherman LS, Legg J, Banine F, Isacke C, Haipek CA, Gutmann DH, Ponta H and Herrlich P. (2001). *Genes Dev.*, **15,** 968–980.
Murthy A, Gonzalez-Agosti C, Cordero E, Pinney D, Candia C, Solomon F, Gusella J and Ramesh V. (1998). *J. Biol. Chem.*, **273,** 1273–1276.
Rouleau GA, Merel P, Lutchman M, Sanson M, Zucman J, Marineau C, Hoang-Xuan K, Demczuk S, Desmaze C and Plougastel B. (1993). *Nature*, **363,** 515–521.
Rusanescu G, Gotoh T, Tian X and Feig LA. (2001). *Mol. Cell. Biol.*, **21,** 2650–2658.
Sainio M, Zhao F, Heiska L, Turunen O, den Bakker M, Zwarthoff E, Lutchman M, Rouleau GA, Jaaskelainen J, Vaheri A and Carpen O. (1997). *J. Cell Sci.*, **110,** 2249–2260.
Schmucker B, Tang Y and Kressel M. (1999). *Hum. Mol. Genet.*, **8,** 1561–1570.
Scoles DR, Chen M and Pulst SM. (2002). *Biochem. Biophys. Res. Commun.*, **290,** 366–374.
Scoles DR, Huynh DP, Chen MS, Burke SP, Gutmann DH and Pulst SM. (2000). *Hum. Mol. Genet.*, **9,** 1567–1574.
Scoles DR, Huynh DP, Mrcos PA, Coulsell ER, Robinson NG, Tamanoi F and Pulst SM. (1998). *Nat. Genet.*, **18,** 354–359.
Shermn L, Xu HM, Geist RT, Saporito-Irwin S, Howells N, Ponta H, Herrlich P and Gutmann DH. (1997). *Oncogene*, **15,** 2505–2509.
Sun CX, Robb VA and Gutmann DH. (2002). *J. Cell Sci.*, **115,** 3991–4000.
Suzuki J, Yamazaki Y, Li G, Kaziro Y and Koide H. (2000). *Mol. Cell. Biol.*, **20,** 4658–4665.
Takaya A, Ohba Y, Kurokawa K and Matsuda M. (2004). *Mol. Biol. Cell*, **15,** 2549–2557.
Thomas G, Merel P, Sanson M, Hoang-Xuan K, Zucman J, Desmaze C, Melot T, Aurias A and Delattre O. (1994). *Eur. J. Cancer*, **30A,** 1981–1987.
Tikoo A, Varga M, Ramesh V, Gusella J and Maruta H. (1994). *J. Biol. Chem.*, **269,** 23387–23390.
Trofatter JA, MacCollin MM, Rutter JL, Murrel JR, Duyao MP, Parry DM, Eldridge R, Kley N, Menon AG and Pulaski K. (1993). *Cell*, **72,** 791–800.
Tsukita S, Yonemura S and Tsukita S. (1997). *Trends Biochem. Sci.*, **22,** 53–58.
Urano T, Emkey R and Feig LA. (1996). *EMBO J.*, **15,** 810–816.
Vojtk AB and Der CJ. (1998). *J. Biol. Chem.*, **273,** 19925–19928.
White MA, Vale T, Camonis JH, Schaefer E and Wigler MH. (1996). *J. Biol. Chem.*, **71,** 16439–16442.
Wolthuis RM, Zwartkruis F, Moen TC and Bos JL. (1998). *Curr. Biol.*, **8,** 471–474.
Yamaguchi A, Urano T, Goi T and Feig LA. (1997). *J. Biol. Chem.*, **272,** 31230–31234.